Evolution in Electrical and Electronic Engineering Vol. 3 No. 1 (2022) 332-340

EEEE

Homepage: http://publisher.uthm.edu.my/periodicals/index.php/eeee
e-ISSN : 2756-8458

Solar PV Tracker System for Traffic Light Application

Wan Nur Sabrina Wan Hazirudin[1], Suriana Salimin[1]*

[1]Faculty of Electrical and Electronic Engineering,
Universiti Tun Hussein Onn Malaysia, Parit Raja, 86400, MALAYSIA

*Corresponding Author Designation

DOI: https://doi.org/10.30880/eeee.2022.03.01.037
Received 21 January 2022; Accepted 29 March 2022; Available online 30 June 2022

Abstract: Solar energy is becoming more essential, particularly in rural areas. However, the conventional photovoltaic cell conversion efficiency is limited. This project will develop a solar PV traffic signal tracker. This study's objective is to track the sun's position. The project has two parts: software and hardware. The device used four light-dependent resistors (LDR) to detect sunlight intensity. The two 180° servo motors are used to move the panel towards the sun. In Proteus, the solar tracker and traffic light system are designed. It was compared to a static solar panel. Finally, the system has shown its potential to gather maximum sunlight.

Keywords: Photovoltaic, Solar Tracker, Traffic Light System

1. Introduction

Solar energy is the most efficient and effective renewable energy source. Solar energy systems are one of the most rapidly evolving renewable energy sources available today. Environmental awareness and energy-saving are factors in the design of solar-powered traffic systems. Traffic lights use solar energy to reduce power usage and optimize renewable energy sources [1]. The proposed technology can regulate traffic both day and night.

An automated system for orienting the panel's surface is required to optimize the output of the solar system. The most noticeable energy production peaks come from perpendicular solar radiation. Numerous authors have created solar photovoltaic trackers to improve the technology's performance [2,3]. In addition to tracking and power generation equipment, they all have a fixed infrastructure [4]. The most efficient solar tracker moves two-axis, azimuth and tilt [4,5].

To construct the solar traffic light, the photovoltaic solar tracker is used. The photovoltaic tracker prototype used Arduino technology and LDR sensors. The tracker's design automatically detects the optimum PV panel direction. When the sun's radiation path is perpendicular to the solar panel, it hits a maximum on the photovoltaic panel. The solar tracking system is required to maximize energy efficiency.

*Corresponding author: suriana@uthm.edu.my

2. Materials and Methods

2.1 Software development

i. Solar tracker

A solar PV tracker system for traffic lights needs to balance power generation and consumption. Batteries supply electricity when solar output is inadequate and store energy when it is needed. Figure 1 shows the Proteus-designed solar tracker simulation circuit.

The sensor data will be digitalized and read in Arduino UNO to compare solar panel orientation. In order to move two servo motors, the Arduino will compute the sun's path. The flowchart below illustrates the solar PV tracker system for traffic signals. Figure 2 shows the solar PV tracker system flowchart.

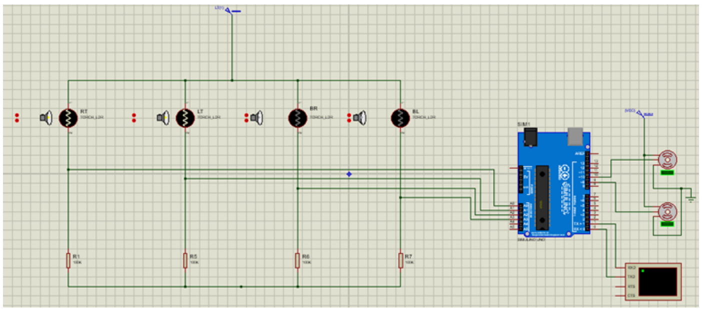

Figure 1: Proteus-designed solar tracker simulation circuit

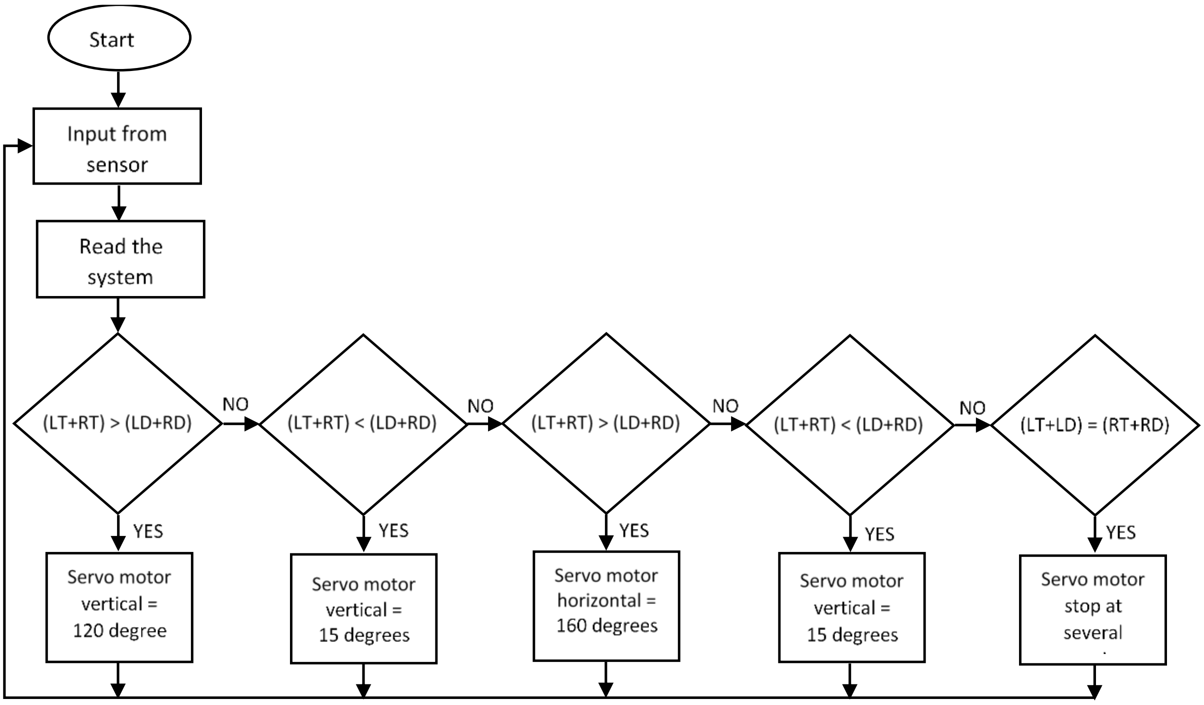

Figure 2: Flow char of Solar PV tracker system

Table 1 tabulates the results of Code Name and function of the sensor. Input from the LDR sensor (A0 to A3) is digitally converted by the Arduino. PWM signals from pin 9 (vertical) and pin 10 (horizontal) operate two 180° servo motors. The LDR sensor data will rotate the servo motor in five different ways in response to the LDR's light intensity from the sun. The Servo motor will rotate between 0° and 120° when the LT and RT sensors detect higher solar radiation. Second, if LT and RT are smaller than LD and RD, the vertical servo motor turns 0 to 15. Third, the horizontal servo motor turns 0 to 160° when the LT and LD sensors' values exceed the RT and RD sensors' values. Finally, when RT and RD sensors are higher than LT and LD, the horizontal motor rotates 0° to 65°. The motor stops when all sensors detect the same quantity of light. It all relies on the sensor's ability to detect sunlight. Finally, the rotational limit was defined based on the solar tracker's maximum and minimum angles during prototype testing.

Table 1: The results of Code Name and function of the sensor

Code Name	Function
LT	Left top
RT	Right top
LD	Left down
RD	Right down

ii.Traffic light

This part will test a 3-way traffic light simulation circuit. The Arduino was used to operate the traffic light simulation circuit. This simulation employed three LED colors to simulate the traffic lights: red, yellow, and green. The first arrangement (pin 8 to 10) will enable lane 1 (the upright circuit) to pass first. The next arrangement (pin 5 to 9) is lane 2 (middle circuit) flow through. Finally, the third arrangement (pin 2 to 4) will allow lane 3 (downright circuit) to flow. Figure 3 shows the proteus-designed solar tracker simulation circuit.

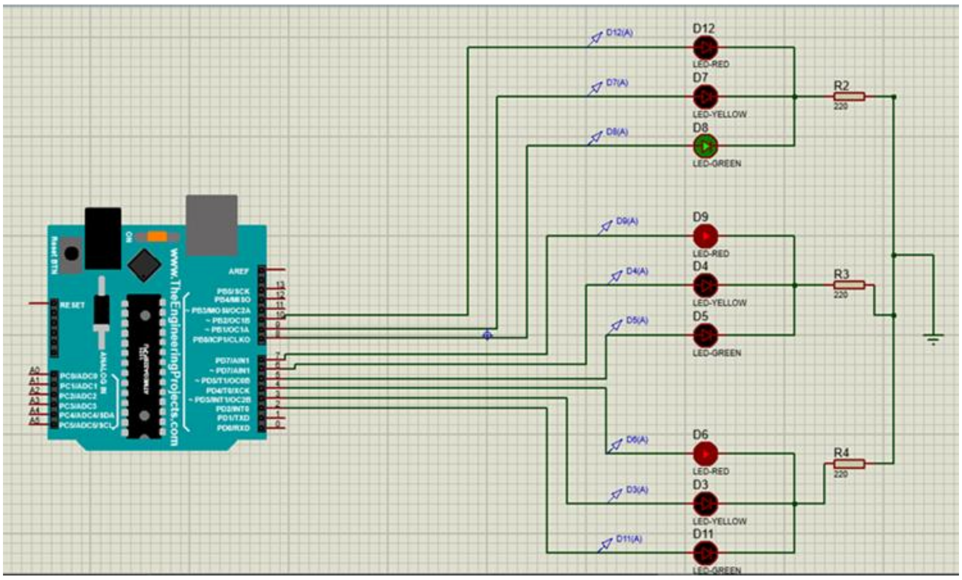

Figure 3: Proteus-designed solar tracker simulation circuit

2.2 Prototype development

The dual-axis solar tracker controlled by Arduino technology is used to develop the solar PV tracker system for traffic lights. The monocrystalline solar panel, traffic light module, 180 servo motor (MG995), battery, and Arduino were used to develop the solar PV tracker system for traffic lights. The concept was to hold and move the solar panel towards the sun. Figure 4 shows the prototype of a solar PV tracker system for traffic lights.

The motor bracket held the servo motor and PV solar panel. The sun tracker used two 180° servo motors to move from east to west and from south to north. Other than that, the box is used as storage for all the components. The partition was made between the sensors to help detect the sun's illumination and work effectively toward the light received between the sensors. The division between LDR is considered a concentrator of radiation and is used to increase the reliability of the solar tracker. As for the traffic light system, the 3-way traffic light with a road prototype has been made to illustrate the entire system.

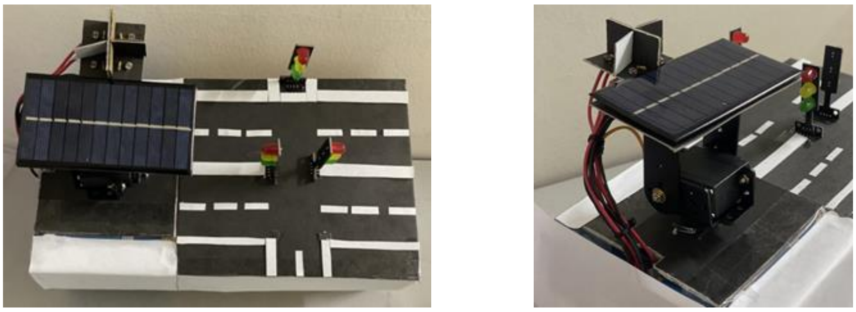

(a) Top view (b) Isometric view

Figure 4: The prototype of a solar PV tracker system for traffic lights

3. Results and Discussion

This chapter will discuss the simulation and result of the solar PV tracker system for traffic light application. The outdoor experiment was conducted in Parit Raja, Johor, Malaysia. The experiment has been tested in two conditions before and after system application. The experiment was conducted from 8:00 am until 06:00 pm.

3.1 Result from simulation

The Proteus software was used to record the simulation result of a solar tracker. The LDR value was calculated in this simulation based on five conditions: average top, average bottom, average left, and average right. Figures 5 illustrate the outcome of a simulation of the solar tracker system's initial condition.

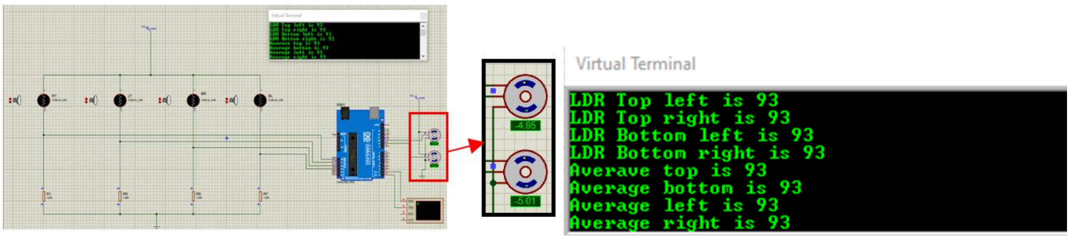

Figure 5: The result simulation in an initial condition

According to Figure 5, the motor's starting position while the LDR is in low condition is 175.05° (horizontal) and 174.99° (vertical). As the LDR value when all LDRs are turned off is 93, the LDR detects no light intensity. Following that, the circuit was tested under average top conditions, with the torch's up arrow pushed for the LDR of the left top (LT) and right top (RT). The torch will approach the LDR sensor and the light emitted by the torch will resemble sunshine. When the LDR detects a change in light intensity, it changes from low to high. Figure 6 show the LDR of LT and RT in high and average top condition**.**

According to Figure 6, the servo motor is positioned horizontally at 174.97 ° and vertically at 90˚. The LT and RT LDR values have been raised from 93 to 1019, showing that both LDRs detect high light intensity. The average top value grew from 93 to 1019. It grew from 93 to 556 while the average value for the bottom stayed constant. Although the left and right averages are increasing, the average top is the highest. In this case, the system's state is decided by the average top, where the servo motor rotates upward. Each simulation phase will be retested using the same method. Figure 7 show the LDR of LD and RD in high and average bottom condition.

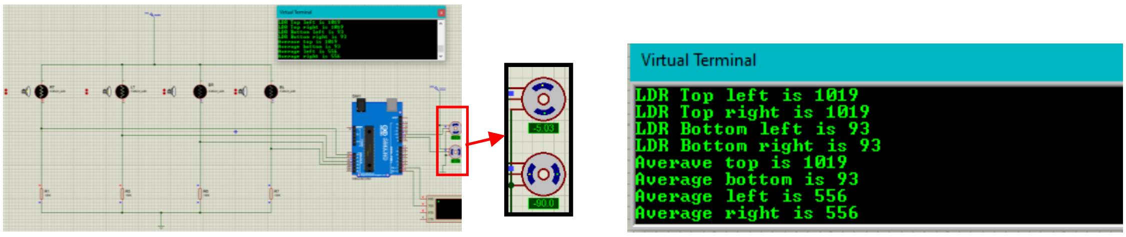

Figure 6: The result simulation of LDR of LT and RT in high and average top condition

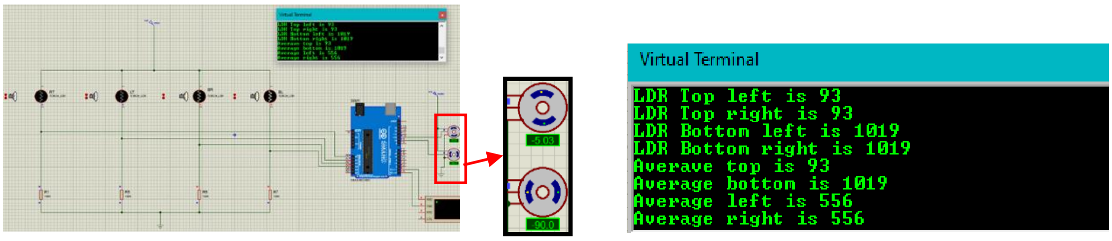

Figure 7: The result simulation of LDR of LD and RD in high and average bottom condition

According to Figure 7, the servo motor is located at 174.97° (horizontal) and 90° (vertical). Now it is obvious that both the LD and RD LDRs detect and respond to light intensity. The average grew from 93 to 1019 points. The left and right averages rise from 93 to 556 while the top average stays at 93. The simulation results show that the bottom average value is higher than the other values. So, the solar tracker's condition was at the average bottom. Vertical servo motors rotate downwards. The simulation then proceeds to test for the average left. Figure 8 show the LDR of LT and LD in high and average left condition.

According to Figure 8, the servo motor is positioned at 126.6° (horizontal) and 175° (vertical). The LDR values of the LT and LD have been increased from 93 to 1019, where it was in high conditions. The average value increased from 93 to 1019. The top and bottom averages increase from 93 to 556 while the right average remains at 93. The simulation result shows that the average value on the left is higher. Due to the high value of the average left, the solar tracker is in the left position. Finally, the last simulation is to test the average right condition. Figure 9 show the LDR of RT and RD in the high and average right condition.

From Figure 9, the servo motor is located at 90° (horizontal) and 175.14° (vertical). The LDR values of the RT and RD have been increased from 93 to 1019, where it was in high conditions. The average value increased from 93 to 1019. Top and bottom average values grow from 93 to 556 while left average values remain at 93. As a result of the simulation, the average value on the right is much greater than the other values. Due to the high value of the average right, the solar tracker's condition is the right position.

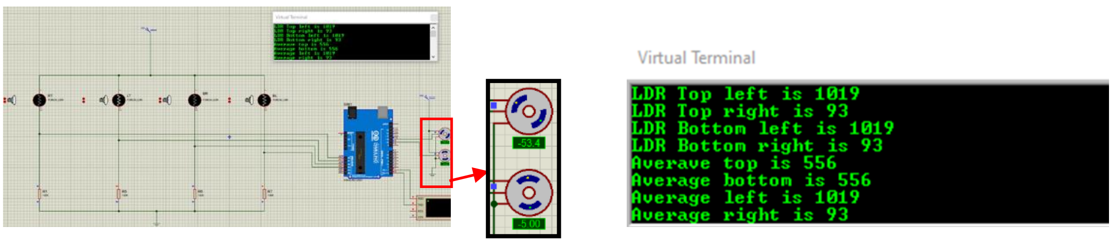

Figure 8: The result simulation of the LDR of LT and LD in high and average left condition

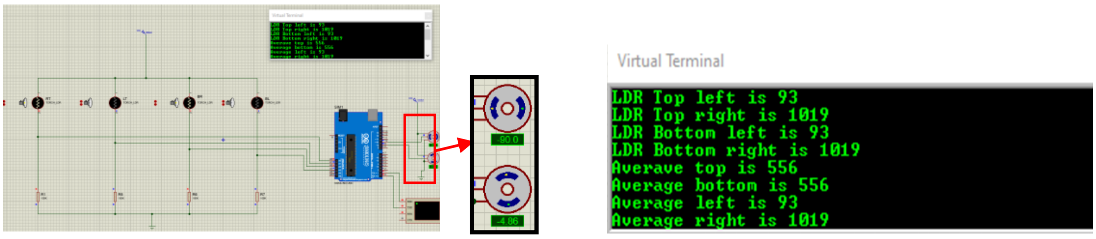

Figure 9: The result simulation of the LDR of RT and RD in high and average right condition

3.2 Result from outdoor experiment

The result of a solar tracker was recorded before and after the system application. The solar panel was used to produce the output such as voltage, current, and power. The table shows the different values of output produced by solar panels before and after the system application. Before the solar tracker application, the solar panel's position was set to the angle of 180°. After the solar tracker application, the solar panel's position will be set according to input from the LDR sensors. Table 2 tabulates the solar panels generated before and after the system application.

Table 2: Result of outdoor experiment

TIME	VOLTAGE (V)		CURRENT (A)		POWER (W)	
	BEFORE	AFTER	BEFORE	AFTER	BEFORE	AFTER
08:00 AM	3.04	3.20	0.01	0.01	0.03	0.03
09:00 AM	3.23	3.48	0.01	0.04	0.03	0.14
10:00 AM	3.50	3.65	0.08	0.11	0.28	0.40
11:00 AM	3.68	3.70	0.11	0.23	0.40	0.85
12:00 AM	3.74	3.81	0.23	0.46	0.86	1.75
01:00 PM	6.30	6.80	0.38	0.55	2.39	3.74
02:00 PM	3.67	3.82	0.13	0.33	0.48	1.26
03:00 PM	3.41	3.63	0.07	0.12	0.24	0.44
04:00 PM	3.39	3.59	0.05	0.12	0.17	0.43
05:00 PM	3.10	3.29	0.02	0.05	0.06	0.16
06:00 PM	2.97	3.00	0.01	0.01	0.03	0.03

Table 2 compares the gain in voltage, current, and power from solar panels before and after using a solar tracker system. The voltage gain by the solar panel before the system application is lower than the voltage gain after the system application. Voltage gain from solar panels is 6.3V and 6.8V, respectively, with the peak of solar radiation around 01:00 pm. However, the panel's voltage output gain is 2.97V and 3.00V for both applications, with the least solar energy around 6:00 pm. The system's power is determined by the solar panel's voltage and current output gains. After gaining the power of solar panels, the percentage of power gained by the solar tracker will be made to show the difference. Table 3 tabulates the percentage of power gained by solar tracker using excel.

Table 3: The percentage of power gained

TIME	POWER (W)		Power gained by the solar tracker (%)
	BEFORE	AFTER	
08:00 AM	0.03	0.03	0.00
09:00 AM	0.03	0.14	78.57
10:00 AM	0.28	0.40	30.00
11:00 AM	0.40	0.85	52.94
12:00 AM	0.86	1.75	50.86
01:00 PM	2.39	3.74	36.10
02:00 PM	0.48	1.26	61.90
03:00 PM	0.24	0.44	45.45
04:00 PM	0.17	0.43	60.47
05:00 PM	0.02	0.16	87.50
06:00 PM	0.03	0.03	0.00

The highest percentage of power gained by the solar tracker is 87.50% from the table above. As for the lowest percentage of power gained, the solar tracker can produce 30%. It shows that the solar tracker can produce the output power from 30% to 87.50% compared to before the application.

3.3 Graph of the experiment data.

The data of the experiment will be recorded and compiled in excel. Next, the graph of voltage against time, current against time, power against time, and percentage of power gained against time will be shown using excel. The graph shows the difference between the output gain before and after the solar tracker application. The graph will be separated according to voltage, current, power, and percentage of power gained. From Figures 10, 11, and 12, the graph slightly increased from 08:00 am until 01:00 pm. After that, the graph fell slightly from 01:00 pm until 06:00 pm. From the graph, the high solar radiation received is from 08:00 am until 01:00 pm and the least after 01:00 pm. After gaining the power value, the percentage of power gained by the solar tracker will be calculated, and the percentage of power gained against time will be plotted.

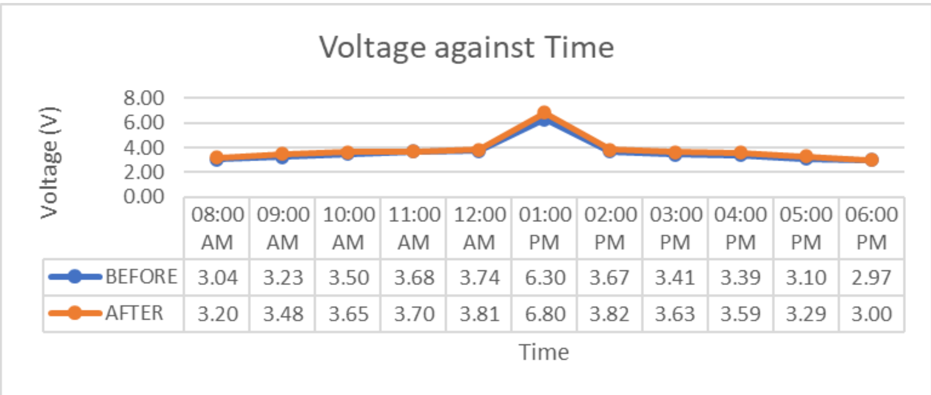

Figure 10: Graph of voltage against time

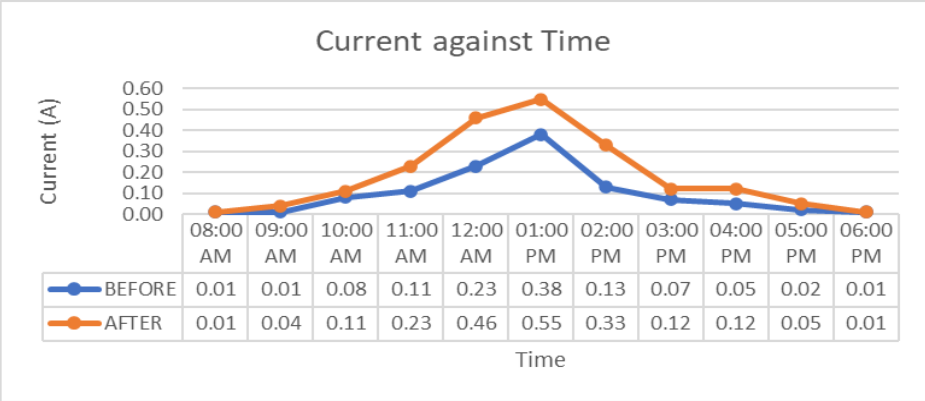

Figure 11: Graph of current against time

Figure 12 shows the graph of the percentage of power gained by the solar tracker against time. The graph shows that the percentage of solar tracker's power is from 30% to 87.50%, where it shows the effectiveness of solar tracker in optimizing the power generation by solar.

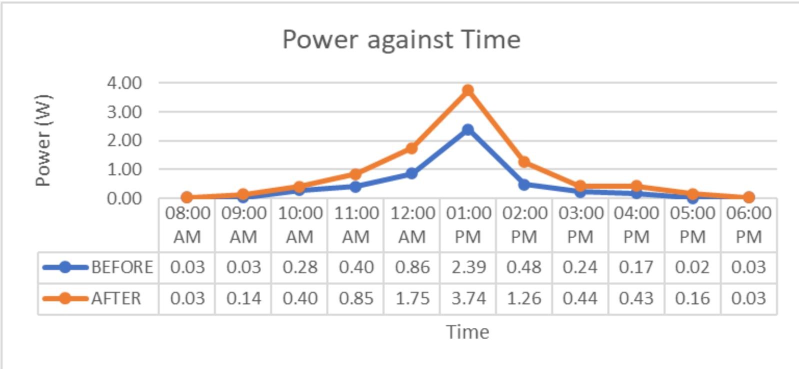

Figure 12: Graph of power against time

Figure 13 shows the graph of the percentage of power gained against time.

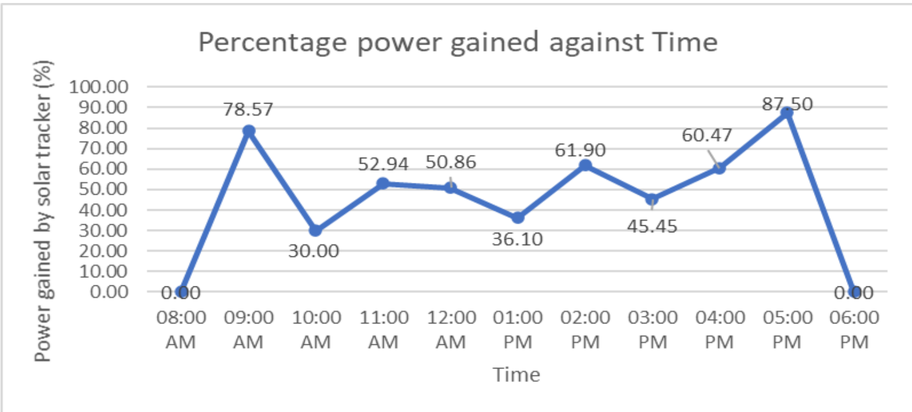

Figure 13: Graph of percentage of power gained against time

4. Conclusion

Based on previous research and analysis done for this project, the conclusion was reached that developing a solar PV tracker system could maximize a photovoltaic system's energy efficiency. Using a low-range solar panel and low-cost electronic components, this solar PV tracker could produce the maximum output gain of the solar system and show the system's effectiveness. Next, the solar tracker can work on dual axes due to the sunlight received by the LDR sensor and was set to the two angles.

The solar tracker can move in two directions, vertical and horizontal, where it can be moved using a 180° servo motor. The solar tracker has been tested towards the sun's direction to determine if the LDR sensor can operate properly. Therefore, this project can improvise by adding the voltage sensor and current sensor module, which can help get better measurements ability than manual measurement using a multimeter.

Acknowledgement

The authors would like to thank the Faculty of Electrical and Electronic Engineering, Universiti Tun Hussein Onn Malaysia for its support.

References

[1] S.R.D. Kalin Gamudali, J.C. Haram Bearach chi, et al; "Pedestrian and vehicular traffic friendly uninterrupted solar-powered traffic signal light system", First International Conference on Industrial and Information Systems, 2006, page: 208.

[2] Quesada, G.; Guillon, L.; Rousse, D.; Mehrtash, M.; Dutil, Y.; Paradis, P.L. "Tracking strategy for photovoltaic solar systems in high latitudes". Energy Convers. Manag.2015,103, 147–156.

[3] Miloudi, L.; Acheli, D.; Ahmed, C. "Solar tracking with a photovoltaic system". Energy Procedia 2013,42, 103–112.

[4] Wang, J.; Lu, C. "Design and Implementation of a Sun Tracker with a Dual-Axis Single Motor for an Optical Sensor-Based Photovoltaic System".Sensors2013,13, 3157–3168 Ingole, A.S. and Rakhonde, B.S., 2015.

[5] Fath Abadi, H. Novel "High efficient offline sensorless dual-axis solar tracker for using in photovoltaic systems and solar concentrators". Renew. Energy2016,95, 485–494